Consistent calculation of the screening and exchange effects in allowed β − transitions

Xavier Mougeot, Charlène Bisch

Consistent calculation of the screening and exchange effects in allowed β^- transitions

X. Mougeot* and C. Bisch

CEA, LIST, Laboratoire National Henri Becquerel (LNE-LNHB), Gif-sur-Yvette, F-91191, France.
(Dated: June 14, 2014)

The atomic exchange effect has previously been demonstrated to have a great influence at low energy in the ^{241}Pu β^- transition. The screening effect has been given as a possible explanation for a remaining discrepancy. Improved calculations have been made to consistently evaluate these two atomic effects, compared here to the recent high precision measurements of ^{241}Pu and ^{63}Ni β spectra. In this paper, a new screening correction has been defined to account for the spatial extension of the electron wave functions. Excellent overall agreement of about 1% from 500 eV to the endpoint energy has been obtained for both β spectra, which demonstrates that a rather simple β decay model for allowed transitions, including atomic effects within an independent particles model, is sufficient to describe well the current most precise measurements.

I. INTRODUCTION

Beta emission probabilities from neutral atoms are highly influenced at low energy by atomic effects, as demonstrated in [1]. The sudden change of the nuclear charge can induce atomic excitations (shake-up) or internal ionizations (shake-off) because initial and final state orbitals are not strictly orthogonal. But the two major atomic effects are the screening and the exchange effects. The latter arises from the creation of a β electron in a bound orbital of the daughter atom corresponding to one which was occupied in the parent atom. An atomic electron from the bound orbital simultaneously makes a transition to a continuum orbital of the daughter atom. This process cannot be distinguished from the direct decay to a final state containing one continuum electron.

At present, precise knowledge of the shape of energy spectra from β transitions, coupled with well-established uncertainties, are sought by end users from the nuclear power industry, the medical care sector ([2],[3]) or for ionizing radiation metrology([4],[5]). These shapes have been little studied since the late 1970s. At that time, the knowledge of the spectral shape was thought to be appropriate. Following this demand, a program to calculate analytically the shape of β spectra for allowed and forbidden unique transitions has already been developed and described elsewhere [6]. This work improves it in calculating exchange and screening effects consistently.

A β spectrum is the product of (i) a weak interaction coupling constant, (ii) a statistical phase space factor pWq^2 which simply reflects the momentum distribution between the electron and the neutrino, (iii) the so-called Fermi function F_0L_0 which corrects for the Coulomb effects, and (iv) a shape factor $C(W)$ which contains all the remaining energy dependencies, such as leptonic and nuclear matrix elements or corrections for atomic effects. Thus, following Behrens' formalism used throughout this work [7]

$$\frac{\mathrm{d}N}{\mathrm{d}W} \quad \propto \quad p \; W \; q^2 \; F_0L_0 \; C(W), \tag{1}$$

with $W = 1 + E/m_e$ the total energy of the electron defined from its kinetic energy E and its rest mass m_e, the corresponding momentum $p = \sqrt{W^2 - 1}$, and the neutrino momentum $q = W_0 - W$ where $W_0 = 1 + E_{\max}/m_e$. The Fermi function, usually denoted by $F(Z, W)$, is

$$F_0L_0 = \frac{\alpha_{-1}^2 + \alpha_1^2}{2p^2}, \tag{2}$$

where the α_κ are the Coulomb amplitudes of the electron radial wave functions, defined in Sec. II B. The parameter κ will be defined in Sec. II.

Denoting (J_i, π_i) and (J_f, π_f) the initial and final nuclear spins and parities, β decays are classified according to $\Delta J = |J_i - J_f|$ and $\pi_i \pi_f$. For allowed and forbidden unique β transitions, the energy dependence of the nuclear matrix elements can be factored out. Introducing $L = 1$ if $\Delta J = 0$ and $L = \Delta J$ otherwise, the shape factor of an allowed ($L = 1$) or an $(L-1)^{\text{th}}$ forbidden unique transition is

$$C(W) = (2L-1)! \sum_{k=1}^{L} \lambda_k \; \frac{p^{2(k-1)} \; q^{2(L-k)}}{(2k-1)![2(L-k)+1]!} \tag{3}$$

with $k = |\kappa|$ and $\lambda_k = \left(\alpha_{-k}^2 + \alpha_k^2\right) / \left(\alpha_{-1}^2 + \alpha_1^2\right)$. These λ_k parameters have to be calculated numerically and the procedure is not straightforward. For this reason, a usual but not justified assumption is to set $\lambda_k \equiv 1$ in classical β spectra calculations, even in the most recent ones [8].

In our previous study [1], the exchange effect was evaluated through Harston and Pyper's formalism [9] using the analytical electron wave functions given by Rose in [10]. A remaining discrepancy was highlighted, possibly due to the usual, but overly simple, screening correction [11]. In the present work, we propose a consistent calculation of these two atomic effects. The continuum and bound orbital electron wave functions have been determined consistently using Behrens' formalism [7], resolving numerically the Dirac equation within an independent particle model. The complete process is given in

---

Sec. II, detailing the structure of the atomic potential for an extended nucleus including screened and exchange potentials. Atomic corrections for allowed β transitions are stated in Sec. III, with a new screening correction for the β spectrum. These calculations are compared to recent precise measurements of the ^{63}Ni and ^{241}Pu β spectra in Sec. IV.

Consistent with Behrens' formalism, natural units $\hbar = m_e = c = 1$ are used throughout this work, except when explicitly specified. All numerical integrations were performed using a three point lagrangian interpolation.

II. ELECTRON WAVE FUNCTIONS

A β^- decay changes a neutron into a proton, ejecting an electron and an antineutrino. The relativistic behaviour of the electron within the Coulomb field of the nucleus is described by the Dirac equation. The Coulomb potential is assumed to be scalar, static and spherically symmetric. The electron wave function can then be split into a radial part and an angular part as [7]

$$\Psi(\vec{r}) = \begin{pmatrix} S_\kappa f_\kappa(r)\chi_{-\kappa}^\mu \\ g_\kappa(r)\chi_\kappa^\mu \end{pmatrix}, \qquad (4)$$

with the electron radial wave functions $f_\kappa(r)$ (small component) and $g_\kappa(r)$ (large component), the spin-angular functions χ_κ^μ, and the sign of κ $S_\kappa = \kappa/|\kappa| = \kappa/k$. κ is the eigenvalue of the operator $\hat{K} = \beta(\vec{\sigma} \cdot \vec{L} + 1)$ which appears by applying the theory of angular momentum to an electron in a Coulomb central field: β is the Dirac matrix, $\vec{\sigma}$ designates the Pauli matrices $\sigma_{x,y,z}$ and $\vec{L}$ is the orbital angular momentum operator. The usual spin-angular functions χ_κ^μ are expanded into the orthonormal basis of the spherical harmonics $Y_l^{\mu-m}$

$$\chi_\kappa^\mu = i^l \sum_m C(l1/2j; \mu - m, m)Y_l^{\mu-m}\chi^m, \qquad (5)$$

with the Clebsch-Gordan coefficients $C(...)$ and the two-component spin eigenfunctions χ^m. $l = k$ and $j = l - 1/2$ if $\kappa > 0$, or $l = k - 1$ and $j = l + 1/2$ if $\kappa < 0$. Notice that the factor i^l in this definition of χ_κ^μ is specific to Behrens' formalism.

The Dirac equation therefore leads to the following system of coupled differential equations

$$\begin{cases} \dfrac{\mathrm{d}f_\kappa}{\mathrm{d}r} = \dfrac{(\kappa - 1)}{r}f_\kappa - [W - 1 - V(r)]g_\kappa \\[2mm] \dfrac{\mathrm{d}g_\kappa}{\mathrm{d}r} = [W + 1 - V(r)]f_\kappa - \dfrac{(\kappa + 1)}{r}g_\kappa \end{cases} \qquad (6)$$

with $V(r)$ a central potential. Beyond free states, analytical solutions for f_κ and g_κ exist only for pure Coulomb potential, i.e. $V(r) = -\alpha Z/r$. Here, Z is the atomic number and α the fine structure constant. These solutions can be found in [10].

Even a slightly more complex description of the nucleus requires a numerical solution. We have followed the method described in detail in [7], where the electron radial wave functions are expressed locally as power series expansions.

A. Atomic potential

The structure of the atomic potential is essential in the determination of the electron wave functions. Its construction is detailed here with our choices regarding the β spectra calculation in which we are interested.

Using Behrens' method [7], a power series expansion of the potential is also needed. Eqs. (6) exhibit two singular points, $r = 0$ and $r = \infty$. Assuming a local C^∞ function, the atomic potential can be expressed locally as a Taylor series, namely, with r_0 denoting an ordinary point,

$$V(r) = \sum_{m=0}^\infty v_m(0)r^m, \qquad r \sim 0 \qquad (7)$$

$$V(r) = \sum_{m=1}^\infty v_m(\infty)r^{-m}, \qquad r \sim \infty \qquad (8)$$

$$rV(r) = \sum_{m=0}^\infty \tilde{v}_m(r_0)(r - r_0)^m, \qquad r \sim r_0 \qquad (9)$$

Notice that in β decay the initial system is a neutral atom and the final system is an ion plus an electron at infinity. The emitted electron thus feels the potential of one elementary charge.

The general structure is the same as depicted in [7], but the required information to perform the calculation is very poorly documented in the literature. We give below all the necessary equations and our choices for the few parameters of this model.

1. Construction

To take into account the finite nuclear size effect in β spectra calculations, the nucleus is decribed as a uniformly charged sphere with nuclear radius R, leading to the usual quadratic behaviour of the potential inside the nucleus. Further, the influence of the atomic electrons has to be taken into account, e.g. through a screened potential. A simple model for a neutral atom has been adopted, well adapted to β decay [7]

$$V(r) = -\frac{\alpha Z}{r}\sum_{i=1}^N a_i e^{-\beta_i r} = -\frac{\alpha Z}{r}\phi(r), \qquad (10)$$

where a_i and β_i are fitted parameters for the considered atom. These parameters have been tabulated many times in the literature. The ones from [12] were chosen in this study because of their completeness and their assumption of independent particles. Using $N = 3$ is sufficient

to represent a screened potential with good accuracy in most applications.

The structure of the atomic potential has to be consistent with the one described by Eqs. (7) to (9) where the space is divided into three parts, and a quadratic behaviour inside the nucleus is required. This potential has to be continuous in any point. A point R_2, sufficiently far away to ensure the convergence of the asymptotic solutions, was introduced. To deal with the exponential part in Eq. (10), a new space region has been defined by introducing a radius R_3. Within $R_3 \leq r \leq R_2$, the remaining charge, which comes from the screened potential, is spread substituting the exponential by a second order polynomial that ensures continuity at R_3 and R_2.

For evaluating the bound states, we have also accounted for the fermion nature of the electrons, which is characterized by exchange symmetry within the many-particle description. An exchange potential, adopted here, has already been introduced by Slater and depends only on the electron charge density by applying the free electron gas assumption [13]. Following Behrens' formalism, this exchange potential is

$$V_{ex}(r) = K \ F_{ex} \ \phi_{ex}^{1/3}(r) \quad \text{with} \tag{11}$$

$$F_{ex} = \frac{3\alpha}{2}\left(\frac{3Z}{4\pi^2}\right)^{1/3}, \quad \phi_{ex}(r) = \sum_{i=1}^{N} a_i \ \frac{\beta_i^2}{r} \ e^{-\beta_i r}. \tag{12}$$

Some Hartree-Fock calculations include a parametrisation of Slater's exchange potential, the convergence process being performed also on these parameters [14]. This possibility has been added to our exchange potential through the adjustment of the constant K (see Sec. II B). Notice that the charge density does not depend upon the atomic orbitals, which might be expected since each orbital does not have the same number of electrons and the same mean radius. The exchange potential can be therefore ajusted for each orbital.

To simplify further notations, we introduce V'_{ex} and ϕ' as the first derivatives of V_{ex} and ϕ, and V''_{ex} and ϕ'' as their second derivatives. All these considerations have led us to define the following atomic potential

$$V(r) = \begin{cases} t_1 + \dfrac{t_2}{2}r^2, & 0 \leq r \leq R \\[2mm] \left(-\dfrac{\alpha Z}{r}\right)\left[C\phi(r) + \delta + \dfrac{C}{\alpha Z} \ rV_{ex} + \delta_{ex}\right], & \\ & R \leq r \leq R_3 \\[2mm] \left(-\dfrac{\alpha Z}{r}\right)\left[1 - C + C\left(\sigma t_3^2 + \mu t_3^3 + \nu t_3^4\right)\right], & \\ & R_3 \leq r \leq R_2 \\[2mm] \left(-\dfrac{\alpha Z}{r}\right)(1 - C), & R_2 \leq r \leq \infty \end{cases} \tag{13}$$

where the following parameters have been defined

$$C = \frac{Z-1}{Z}, \quad \delta_{ex} = -\frac{CR}{\alpha Z}\left[2V_{ex}(R) + RV'_{ex}(R)\right],$$

$$\eta = \sum_i a_i \left[1 - (1 + \beta_i R)e^{-\beta_i R}\right], \quad \delta = 1 - C + C\eta,$$

$$t_1 = \left(-\frac{3\alpha Z}{2R}\right)\left[1 + \frac{2}{3}CR\phi'(R) + \frac{2}{3}\delta_{ex}\right],$$

$$t_2 = \left(\frac{\alpha Z}{R^3}\right)\left[1 - \frac{2CR}{\alpha Z}V_{ex}(R)\right],$$

$$t_3 = \frac{r - R_2}{R_3 - R_2}, \quad \sigma = \frac{D_2}{2} - 3D_1 + 6D_0,$$

$$\mu = -D_2 + 5D_1 - 8D_0, \quad \nu = \frac{D_2}{2} - 2D_1 + 3D_0,$$

$$D_0 = \phi(R_3) + \eta + \frac{R_3}{\alpha Z}V_{ex}(R_3) + \frac{\delta_{ex}}{C},$$

$$\frac{D_1}{R_3 - R_2} = \phi'(R_3) + \frac{V_{ex}(R_3) + R_3 V'_{ex}(R_3)}{\alpha Z},$$

$$\frac{D_2}{(R_3 - R_2)^2} = \phi''(R_3) + \frac{2V'_{ex}(R_3) + R_3 V''_{ex}(R_3)}{\alpha Z}. \tag{14}$$

The first derivative of $V(r)$, also continuous, and the second derivative, have been established by straightforward calculations. The potential for continuum states is simply obtained by setting all the exchange terms to zero in Eqs. (13) and (14).

The parameters R_2 and R_3 influence the shape of the atomic potential. For $r \geq R_2$, an electron in a continuum state feels the potential of a unique charge. Thus, R_2 is a kind of atomic radius. The authors of [7] do not provide any specific criterion to set R_2 and R_3. Being inspired by [15], these parameters have been set to $R_2 = 350(W/p)$ and $R_3 = 150(W/p)$. No convergence problem of the asymptotic solutions was noticed in our study.

Validity of the asymptotic solutions of the bound states, beyond R_2, can be closer than for the continuum states when considering inner orbitals. To speed up the calculation, these parameters have been set differently for the bound states. The radius R_2 has been determined as the smallest radius for which the asymptotic solutions of the considered orbital converges. The radius R_3 has been empirically set to $R_3 \sim R_2/2$ in order to smooth the reconnection to the asymptotic potential.

2. Usable form for calculation

Particular attention has to be paid when going from the potential of Eq. (10) to the potential defined in Eqs. (7) to (9). For the continuum states, the atomic potential with screened potential but no exchange potential is

needed. The following helpful relation was used

$$\mathrm{e}^{-\beta r} = \mathrm{e}^{-\beta r_0} \sum_{m=0}^{\infty} \frac{1}{m!}(-\beta)^m (r - r_0)^m. \qquad (15)$$

The v_m coefficients have been established within the different space regions, in $0 \leq r \leq R$

$$V(r) = \sum_{m=0}^{2} v_m r^m \text{ with } v_0 = t_1, \ v_1 = 0, \ v_2 = \frac{t_2}{2}, \quad (16)$$

in $R \leq r \leq R_3$

$$rV(r) = \sum_{m=0}^{\infty} v_m (r - r_0)^m \text{ with}$$
$$v_0 = (-\alpha Z)\left(\delta + C \sum_i a_i \mathrm{e}^{-\beta_i r_0}\right), \qquad (17)$$
$$v_m = (-\alpha Z) C \sum_i a_i \mathrm{e}^{-\beta_i r_0} \frac{(-\beta_i)^m}{m!} \quad \forall m > 0,$$

in $R_3 \leq r \leq R_2$

$$rV(r) = \sum_{m=0}^{4} v_m (r - r_0)^m \text{ with}$$
$$v_0 = (-\alpha Z)[1 - C + CU_0], \qquad (18)$$
$$v_m = (-\alpha Z) C U_m \quad \forall m > 0,$$

where $R_d = r_0 - R_2$, $t_4 = \dfrac{R_d}{R_3 - R_2}$, $U_0 = \sigma t_4^2 + \mu t_4^3 + \nu t_4^4$,

$$U_1 R_d = 2\sigma t_4^2 + 3\mu t_4^3 + 4\nu t_4^4, \quad U_2 R_d^2 = \sigma t_4^2 + 3\mu t_4^3 + 6\nu t_4^4,$$

$$U_3 R_d^3 = \mu t_4^3 + 4\nu t_4^4, \qquad U_4 R_d^4 = \nu t_4^4,$$

and in $R_2 \leq r \leq \infty$

$$V(r) = v_1 r^{-1} \text{ with } v_1 = -\alpha. \qquad (19)$$

For the bound states, the parameter v_1 is identical in $[R_2, \infty[$. The v_m coefficients within $[0, R]$ and $[R_3, R_2]$ remain the same provided that the parameters t_1, t_2, D_0, D_1 and D_2 are evaluated by taking the exchange potential into account.

In $[R, R_3]$, a specific treatment is required because of the $r^{-1/3}$ behaviour. In this study, an exact evaluation of the potential was implemented. Eq. (9) is just the Taylor series of any function $f(r)$ in the vinicity of r_0. Thus we can define

$$\sum_{m=0}^{\infty} \frac{f^{(m)}(r_0)}{m!}(r - r_0)^m = \sum_{m=0}^{\infty} \tilde{v}_m(r_0)(r - r_0)^m. \quad (20)$$

The three first terms of this series are trivial. The residual can be calculated exactly since the exact values of the potential and its derivatives are known

$$\mathrm{Res} = rV(r) - \sum_{m=0}^{2} \frac{f^{(m)}(r_0)}{m!}(r - r_0)^m. \qquad (21)$$

A final third order term is therefore added, identifying $\mathrm{Res} \equiv v_3(r_0)(r - r_0)^3$. This cubic term of the series is not exact, but the calculated potential is exact and the polynomial exhibits an appropriate behaviour up to at least $m = 2$. Of course, this requires a dense enough r grid to have a small residual. In practice, this residual is about $10^{-4}\%$ and always less than 0.1%.

B. Radial wave functions

In Behrens' method [7], the electron radial wave functions are expressed locally as power series expansions, allowing Eqs. (6) to be solved using recurrence relations. Special treatment is needed for the solutions relative to the regular singular point $r = 0$, and for the asymptotic solutions relative to the irregular singular point $r = \infty$. Then, the calculation consists in evaluating the wave functions near $r = 0$, near $r = \infty$, and step by step between these two points in order to reconnect each solution with the appropriate renormalisation and phase shift. Coulomb amplitudes α_κ are given, and defined, by the reconnection of the solutions near $r = 0$ with the ordinary solutions. They are linked to the values of the radial wave functions at the nuclear radius. Similarly, the phase shifts are given by the reconnection of the asymptotic solutions with the ordinary solutions.

In order to be sure of our calculations for the continuum wave functions, the tables from [16] of various parameters used to calculate β spectra were recalculated. Unscreened Coulomb functions (Table II in [16]) were perfectly reproduced, and the ratios of screened to unscreened Coulomb functions (Table III in [16]) were in very good agreement for all Z. Incidently, this allows us to calculate these parameters at any desired energy, especially the λ_k parameters involved in the shape factors of Eq. (3), avoiding any interpolation in these tables.

For the bound wave functions, the procedure is basically the same but the orbital energy T is not known in advance. An iterative procedure is needed which has to start with a relatively good initial energy to ensure a quick convergence toward the actual energy.

Behrens and Bühring have proposed a Newton iteration method [7], used in this study. Starting from the analytical energy T_0 given in [10], the zeros of the following estimator have to be found

$$D(T) = g_R(r_M) f_L(r_M) - g_L(r_M) f_R(r_M) \qquad (22)$$

with $r_M = \gamma(\gamma + n')/\alpha Z$, using the recurrence relation

$$T_{n+1} = T_n - D(T)/\dot{D}(T), \qquad (23)$$

with $\dot{D}(T)$ the first derivative of this estimator. Our calculation stops when $|T_n - T_{n-1}| < 10^{-13}$.

This procedure is not sufficient because the power series expansions of the wave functions do not depend explicitly on the main quantum number n, but only on κ.

Thus, for the same value of κ, several convergence energies are possible. The number of nodes of f_κ and g_κ have therefore to be checked to select the desired orbital.

The orbital energy determines the oscillation frequency of the radial wave functions. As an overlap between the bound and continuum wave functions is needed for the exchange effect, good accuracy of the orbital energy is required. Significant discrepancies have been found for low lying orbitals using the procedure detailed just above. An additional procedure has thus been implemented in order to ensure good convergence. The one electron energies E_{Des} of Desclaux in [17] have been choosen for their completeness and for the quality of the calculations. The K constant parameter of the exchange potential in Eq. (11) is adjusted by dichotomy inside an empirical interval $K_{\min} = -2$ and $K_{\max} = 2$. The convergence is reached in about 10 iterations, when the orbital energy is close to E_{Des} at the 0.01% level, with a minimum of 0.1 eV. Finally, notice that this method is generic in the sense that the tabulated energies from [17] can be changed to experimental ones, for instance.

To verify our calculations, the parameters of Table V from [16] for the bound wave functions, useful in electron capture calculations, were recalculated. Good agreement for all Z has been obtained. The Coulomb amplitudes of the bound wave functions given in Table IX by Bambynek *et al.* [18] were also recalculated and good agreement has also been achieved.

III. ATOMIC EFFECTS ON β SPECTRA

A. Exchange effect

The formalism of the exchange effect has already been set out in detail in [19]. For allowed transitions, only β electrons created in an s bound orbital of the daughter atom can take part. This effect is expressed as a correction factor $\left[1 + \eta_{ex}^T(E)\right]$ which modifies the β spectrum defined in Eq. (1). The total exchange factor $\eta_{ex}^T(E)$ depends on the β electron energy E and involves an overlap between the electron radial wave functions of the bound and continuum orbitals. It can be written in terms of the subshell contributions η_{ex}^{ns}

$$\eta_{ex}^T(E) = \sum_n \eta_{ex}^{ns}(E) + \sum_{\substack{m,n \\ (m \neq n)}} \mu_m \mu_n, \qquad (24)$$

and the exchange factor of the n-th subshell is given by

$$\eta_{ex}^{ns}(E) = f\left(\mu_n^2 - 2\mu_n\right). \qquad (25)$$

The parameters μ_n and f are expressed using the bound $(f_{n,\kappa}^b, g_{n,\kappa}^b)$ and continuum (f_κ^c, g_κ^c) electron radial wave functions evaluated at the nuclear radius according to

$$\mu_n = \langle Es'|ns \rangle \frac{g_{n,\kappa}^b(R)}{g_\kappa^c(R)}, \quad f = \frac{g_\kappa^c(R)^2}{g_\kappa^c(R)^2 + f_\kappa^c(R)^2}. \qquad (26)$$

For s orbitals, $\kappa = -1$. $\langle Es'|ns \rangle$ is the overlap between the initial bound orbital of the parent atom $|ns\rangle$ and the final continuum orbital of the daughter atom $\langle Es'|$ over the entire space.

In contrast with our previous study [1] and the study in [9], here the screened electron wave functions for both the continuum and bound states have been determined in a complete and consistent manner.

B. A new screening correction

When calculating a β spectrum, the screening effect is generally corrected for using a constant Thomas-Fermi potential which is subtracted from the total energy of the particle [11]. This method creates a non-physical discontinuity at the minimum energy defined by the Thomas-Fermi potential [6]. This minimum energy is $\lesssim 20$ keV, hence the discontinuity does not generally affect the practical use of the spectrum. Physically, the influence of the atomic electrons is expected to be significant when the β wavelength is comparable to the atom size, *i.e.* at low energy. As it has been shown in [1], this simple method, which allows analytical wave functions to be used, cannot be reasonable for high Z and at low energy.

Beta spectra are classically calculated using the electron radial wave functions evaluated at the nuclear radius. To take the screening into account, it is not just sufficient to renormalise the wave functions and evaluate them at the nuclear radius because the screened potentials are very weak at this distance, and so, the modification is completely negligible over the entire range of the spectrum. For example, in the case of ^{241}Pu and using the parameters given in [12], one can evaluate $[1 - \phi(R)] = 7.24 \cdot 10^{-6}$.

It is, in fact, necessary to take into account the spatial extension of the wave functions. As described in [7], this can be done by evaluating the transition matrix of the corresponding β decay. However the calculations become very complicated because the electron wave functions are coupled with the nuclear matrix elements involved. To avoid this difficulty, we can benefit from the parameter f defined in Eq. (26) for the exchange effect. This parameter represents the fraction of β electrons which emerge in a continuum κ state if the exchange process is omitted. Instead of squared wave functions evaluated at the nucleus surface, the mean value of the squared radial wave functions over the entire space has been used

$$\overline{g_\kappa^2} = \frac{1}{\Delta R} \int_{\Delta R} g_\kappa^2(r) dr, \qquad (27)$$

where ΔR is the effective integration interval. The correction factor that takes the screening into account is

$$C_{sc} = 1 - \frac{\Delta R_{unsc}}{\Delta R_{sc}} \cdot \left(1 - \frac{f_{sc}}{f_{unsc}}\right), \qquad (28)$$

where the subscript sc ($unsc$) means that the screened (unscreened) wave functions were used. In this way, the

screening correction is physically meaningful because of the definition of the Fermi function in Eq. (2).

C. Numerical procedure

The calculation of the exchange effect is performed in two stages. First, the bound wave functions have to be calculated and stored. The minimal sampling that corresponds to the adaptive step given in [7] is used for the r grid. The continuum wave functions are calculated at the desired energies in the final β spectrum, with their own adaptive r grids. Next, the overlap between the bound and continuum wave functions can be determined, and thus the contribution of each orbital and the total correction factor for the exchange effect.

To perform the calculation of the overlap, the bound and continuum r grids are concatenated and the wave functions are evaluated at these new points. However, if the common grid is not sufficiently dense, numerical fluctuations appear in the overlap calculation, and thus in the final β spectrum. In practice, we observed that a refined grid with just one more point between each point of the common grid is sufficient to ensure good convergence with a precision $\lesssim 10^{-3}\%$.

IV. RESULTS

Accurate calculations, based on inclusion of the various effects covered above, have been performed for the allowed transition of ^{63}Ni and the first forbidden non-unique transition of ^{241}Pu. Radiative corrections have also been included but their influence on the β spectrum is negligible, as shown in [6].

^{63}Ni decays entirely by β^- emission to the ground state of ^{63}Cu. This allowed transition has an endpoint energy of $E_{\max} = 66.980$ (15) keV [20]. ^{241}Pu decays mainly by β^- emission to the ground state of ^{241}Am. This first forbidden non-unique transition, with $E_{\max} = 20.8$ (2) keV [21], fulfills the assumption of the ξ approximation and can be calculated as allowed [22], as it has been proved in [1].

The low maximum energies of these two transitions make them ideal cases for evaluating the influence of the atomic effects. The β spectra of ^{63}Ni [23] and ^{241}Pu [24] were recently measured using metallic magnetic calorimeters. Each source was enclosed in a gold absorber assuring a 4π solid angle and 100% detection efficiency. These spectra are first compared to classical β calculations, and then taking into account the screening and exchange effects. The theoretical spectra were normalized to the data by integration from 500 eV to $E_{\max}$ for both ^{63}Ni and ^{241}Pu decays, for being as much as possible independent of the statistical fluctuations of the measurement.

A. A simple statistical analysis

To evaluate the global quality of our theoretical spectra, some simple elements of statistical analysis are proposed. For a set of n measurements $\{y_i\}$, the fit quality of a model, leading to n predictions $\{y_i^{th}\}$, with respect to the data is given by the quantity

$$R^2 = 1 - \frac{\text{var}(\hat{e}_i)}{\text{var}(y_i)}. \tag{29}$$

Valid for $n \gg 1$, this definition is general, without any restriction on the type of model. This quantity falls in $0 \leq R^2 \leq 1$, where $R^2 = 1$ corresponds to perfect predictions. The modeling error is $\hat{e}_i = y_i - y_i^{th}$. Non biased estimators of the variances are

$$\text{var}(y_i) = \sum_{i=1}^{n} \frac{(y_i - \overline{y})^2}{n-1}, \quad \text{var}(\hat{e}_i) = \sum_{i=1}^{n} \frac{(\hat{e}_i)^2}{n-p-1} \tag{30}$$

with $\overline{y}$ the simple mean of the measurements, and p the number of parameters of the model. For β spectra, $p = 2$ was considered, namely the maximum energy of the transition and the normalisation of the theoretical spectrum to the data. Therefore, the coefficient $(1 - R^2)$ quantifies the general disagreement between the measurements and the predictions.

For the end user, this criterion does not provide any information about the uncertainty of the emission probability at a given energy. We propose first to look at the distribution of the standardized residuals

$$r_i = \frac{\hat{e}_i}{\sqrt{\text{var}(\hat{e}_i)}}. \tag{31}$$

If these residuals are almost equally distributed around zero, it is appropriate to assume that they are distributed according to a Gaussian probability variance $\text{var}(r_i)$. The standard deviation $\sigma_{r_i} = \sqrt{\text{var}(r_i)}$ then gives an estimate of the overall uncertainty of the calculated spectrum in the energy range where the measurements exist. Notice that this analysis is not relevant if the standardized residuals are not equally distributed.

Given the energy thresholds of the measured β spectra considered in this study, these statistical parameters have been calculated from 500 eV to the maximum energy of the transition for both ^{63}Ni and ^{241}Pu.

B. ^{63}Ni beta spectrum

Fig. 1 presents the total exchange factor η^{tot} for the ^{63}Ni decay, with the contribution of each orbital η^{ns}. These results are consistent with those calculated in the framework described in [1] where relativistic analytical wave functions and relativistic effective nuclear charges had been used. Both in this previous framework and the present one, a partial negative contribution of one orbital

was found, creating a maximum in the total exchange factor of 10.7% at 500 eV for this study.

Fig. 2 compares the experimental spectrum with three theoretical predictions: an analytical β calculation, without screening and exchange; a numerical calculation from this work, with screening but without exchange; a complete numerical calculation with screening and exchange. Notice that the endpoint energy from the measured spectrum is $E_{max} = 67.176$ (173) keV [23]. This value disagrees with the lastest evaluated one [20]. The latter value comes from mass measurements and is therefore well known. The value from [23] probably points out some small non linear effects of about 0.1% that were not taken into account within the data analysis. Nevertheless, this spectrum is the only one available of such high quality at low energy. These two endpoint energies were tested and the results did not change significantly.
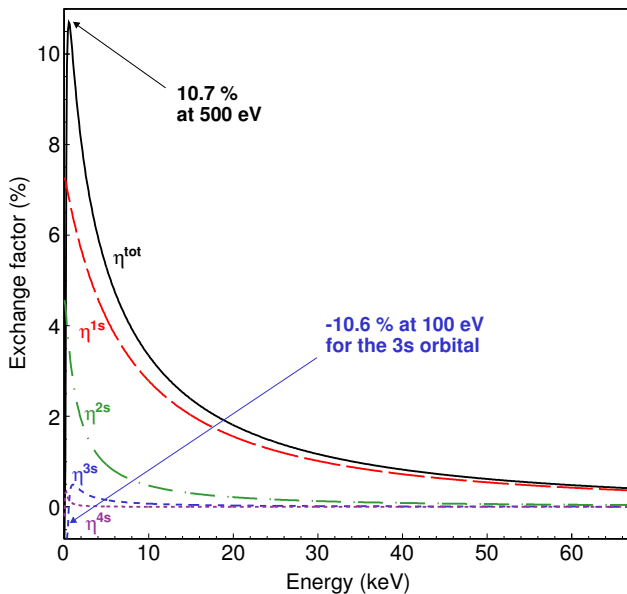

FIG. 1. (Color online) Total exchange factor η^{tot} for the ^{63}Ni decay, with the contribution of each orbital η^{ns}.

Eventually, an excellent agreement has been obtained with the experimental spectrum if the screening and exchange effects are taken into account. The standardized residuals are equally distributed around a mean value of $\bar{r} = 0.093\%$. The standard deviation of the residuals is $\sigma_{r_i} = 1.03\%$ and the global disagreement is $(1 - R^2) = 0.028\%$. The discrepancy between 500 eV and the energy threshold of the measurement at 200 eV comes directly from the influence of the $3s$ orbital in our calculation, but it is difficult to know if it is due to the experiment or to the model. Mean energies are also interesting quantities: $\overline{E}_{an} = 17.45$ keV for the analytical calculation; $\overline{E}_{sc} = 17.40$ keV for the numerical calculation with screening; $\overline{E}_{scex} = 17.14$ keV for the complete

calculation. As expected, the screening effect is weak for this low Z nucleus, but the exchange effect is of importance, as is confirmed experimentally.
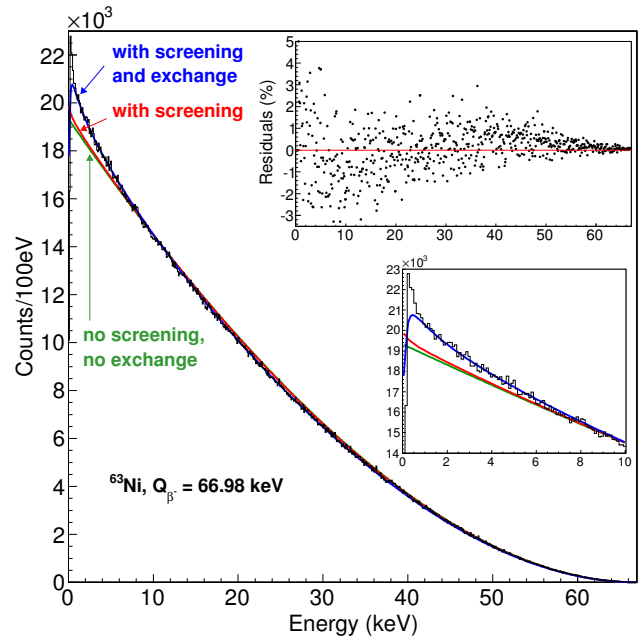

FIG. 2. (Color online) Measured ^{63}Ni β spectrum compared to analytical calculation (green), numerical calculation with screening (red), and numerical calculation with screening and exchange (blue). Normalization to the data was done by integration from 500 eV to E_{max}. Standardized residuals between the data and the most complete calculation are also given. A zoom on the low energy region is also given.

C. ^{241}Pu beta spectrum

Fig. 3 presents the total exchange factor η^{tot} for ^{241}Pu decay, with the contribution of each orbital η^{ns}. These results are consistent with those calculated in the framework described in [1]. The total exchange factor is more pronounced in this study, with a higher contribution of the inner orbitals. Fig. 4 compares the experimental spectrum with the same three theoretical predictions as for the ^{63}Ni spectrum. The fall of the experimental spectrum between 500 eV and the energy threshold of the measurement at 300 eV is most likely due to the data analysis. Excellent agreement has been obtained with the experimental spectrum if the screening and exchange effects are taken into account. The standardized residuals are equally distributed around a mean value of $\bar{r} = 0.0019\%$. The global disagreement is $(1 - R^2) = 0.040\%$ and the standard deviation of the residuals is $\sigma_{r_i} = 0.99\%$. For the mean energies, we find $\overline{E}_{an} = 5.24$ keV, $\overline{E}_{sc} = 5.18$ keV and $\overline{E}_{scex} = 5.03$ keV. As expected, the screening effect is strong for this high

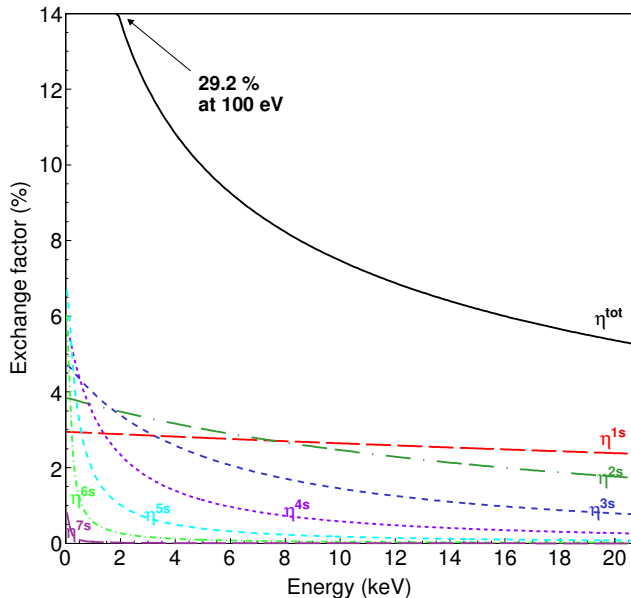Z nucleus, equivalent to the magnitude of the exchange effect, as is confirmed experimentally.

FIG. 3. (Color online) Total exchange factor η^{tot} for the ^{241}Pu decay, with the contribution of each orbital η^{ns}.

V. CONCLUSION

A consistent calculation of the screening and exchange effects in allowed β^- transitions has been given in detail. The exchange effect has been determined with Harston and Pyper's formalism [9], but using more precise relativistic electron wave functions calculated within Behrens' formalism [7]. Special care has been taken to explain the details of these calculations because of the lack of information available in the literature.

This work has demonstrated that a rather simple calculation within an independent particles model is sufficient to obtain a fine understanding of the atomic effects that occur in β decays. A new screening correction that accounts for the spatial extension of the electron wave functions has had to be defined to reach the required precision due to the high quality of the measurements used for comparison. Excellent overall agreement of about 1% from 500 eV to the endpoint has been obtained for both the β spectra of ^{63}Ni and ^{241}Pu decays. Even though more complex calculations, such as multiconfigurational Dirac-Fock ones, can take into account chemical effects through ionised atomic states, they are not deemed nec-

essary due to the current precision of β spectra measurements.

Finally, this work allows the exact calculation of the leptonic matrix elements within Behrens' formalism. The obvious next step, on which we are currently working, is to generalize the screening and exchange corrections to forbidden unique transitions, which can be performed without taking into account the nuclear matrix elements. A longer term goal is the generalization to forbidden non-unique transitions, which will inherently require the calculation of the nuclear matrix elements. All these new calculations will be compared to existing and available new measurements.
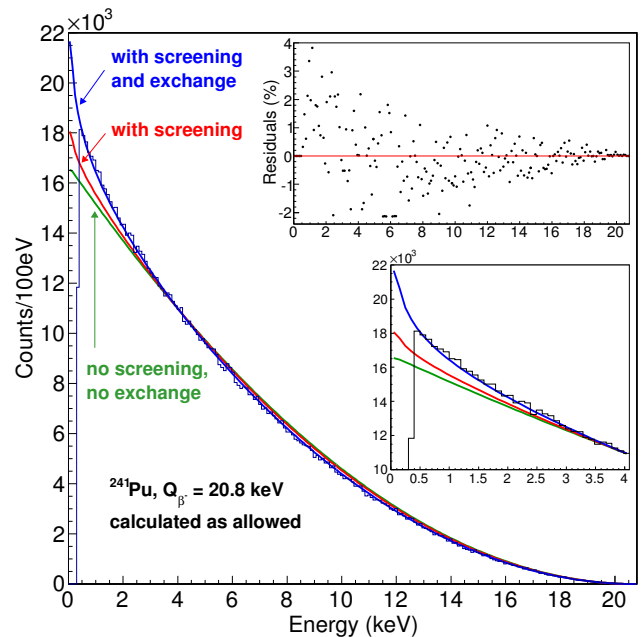

FIG. 4. (Color online) Measured ^{241}Pu β spectrum compared to analytical calculation (green), numerical calculation with screening (red), and numerical calculation with screening and exchange (blue). Normalization to the data was done by integration from 500 eV to E_{max}. Standardized residuals between the data and the most complete calculation are also given. A zoom on the low energy region is also given.

[1] X. Mougeot *et al.*, Phys. Rev. A **86**, 042506 (2012).

[2] M. Bardiès and J.-F. Chatal, Phys. Med. Biol. **39**, 961 (1994).

[3] A. I. Kassis, Int. J. Radiat. Biol. **80**, 789 (2004).

[4] R. Broda, P. Cassette, and K. Kossert, Metrologia **44**, S36 (2007).

[5] C. Bobin *et al.*, Appl. Radiat. Isot. **68**, 2366 (2010).

[6] X. Mougeot *et al.*, in *LSC2010*, edited by P. Cassette, Radiocarbon (University of Arizona, 2010) pp. 249–257.

[7] H. Behrens and W. Bühring, *Electron radial wave functions and nuclear beta decay* (Oxford Science Publications, 1982).

[8] P. Huber, Phys. Rev. C **84**, 024617 (2011).

[9] M. R. Harston and N. C. Pyper, Phys. Rev. A **45**, 6282 (1992).

[10] M. E. Rose, *Relativistic electron theory* (Wiley and Sons, 1961).

[11] R. H. Good, Phys. Rev. **94**, 931 (1954).

[12] F. Salvat *et al.*, Phys. Rev. A **36**, 467 (1987).

[13] J. C. Slater, Phys. Rev. **81**, 385 (1951).

[14] I. P. Grant, Adv. Phys. **19**, 747 (1970).

[15] W. Bühring, Nucl. Phys. **61**, 110 (1965).

[16] H. Behrens and J. Jänecke, *Landolt-Börnstein, New Series, Group I, vol. 4* (Springer Verlag, Berlin, 1969).

[17] J. P. Desclaux, At. Data Nucl. Data Tables **12**, 311 (1973).

[18] W. Bambynek *et al.*, Rev. Mod. Phys. **49**, 77 (1977).

[19] N. C. Pyper and M. R. Harston, Proc. Roy. Soc. Lond. A **420**, 277 (1988).

[20] M.-M. Bé *et al.*, in *Table of Radionuclides – Monographie BIPM-5*, Vol. 3, edited by CEA/LIST-LNHB (BIPM, ISBN 92-822-2218-7, 2006) pp. 29–31.

[21] M.-M. Bé *et al.*, in *Table of Radionuclides – Monographie BIPM-5*, Vol. 4, edited by CEA/LIST-LNHB (BIPM, ISBN 92-822-2230-6, 2008) pp. 259–267.

[22] H. F. Schopper, *Weak interactions and nuclear beta decay* (North-Holland Publishing Company, 1966) p. 284.

[23] C. Le-Bret, *PhD thesis* (Université Paris 11, 2012).

[24] M. Loidl *et al.*, Appl. Radiat. Isot. **68**, 1460 (2010).